Brazilian Journal
of Chemical
Engineering

ISSN 0104-6632
Printed in Brazil
www.abeq.org.br/bjche

Vol. 32, No. 01, pp. 225 - 235, January - March, 2015
dx.doi.org/10.1590/0104-6632.20150321s00002732

NOVEL SIMILARITY-SOLUTION WHICH IS APPLICABLE FOR FREE CONVECTION OVER A BODY OF ARBITRARY SHAPE: THERMAL NON-EQUILIBRIUM IN A POROUS MEDIUM

M. M. Shahmardan, M. Nazari* and A. A. Samani

Department of Mechanical Engineering, University of Shahrood, Shahrood, Iran.
P.O. Box 3619995161, Phone: + 989122730243
E-mail: nazari_me@yahoo.com

(Submitted: May 26, 2013 ; Revised: February 7, 2014 ; Accepted: April 7, 2014)

Abstract - The study of the natural convection flow and heat transfer from hot surfaces in a porous medium has been of considerable interest in energy-related engineering problems. This paper is concerned with the free convection heat transfer over an *arbitrary* hot surface in a porous medium. It is assumed that the fluid and solid phases are not in local thermal equilibrium and therefore a two-temperature model of heat transfer is applied. The coupled momentum and energy equations are used and transformed into ODE's. The similar equations obtained are solved numerically and the local heat flux is shown for three types of axisymmetric shapes, i.e., a vertical plate, horizontal cylinder and sphere. The results have also been validated with the available results in the literature; which show that our assumptions and numerical method are accurate. Mathematical derivation of a similarity solution for an arbitrary geometry in the heat transfer analysis is the main novelty of the present study.
Keywords: Similarity Solution; Arbitrary Surface; Porous Medium; Natural Convection.

INTRODUCTION

The study of the natural convection flow and heat transfer from hot surfaces in a porous medium has been of considerable interest in energy-related engineering problems for many decades. A pioneering study by Cheng and Minkowycz (1977) investigated convection induced by a hot vertical surface. The great majority of papers which have studied such problems usually have adopted a single field equation for the temperature field of the porous medium. But a very recent work has been concerned with relaxing the assumption that the local temperatures of the solid and fluid phases are equal. A simple example where this situation might arise is when a hot fluid is suddenly injected into a cold porous medium, and it takes time for the mean temperatures of the phases at any chosen point to tend towards the same value; see for example Rees *et al*. (2008) and Rees and Bassom (2010). Furthermore, such a lack of local thermal equilibrium is not confined to unsteady configurations. Steady state examples include cavity convection studied by Baytaş and Pop (2002) and Mohamad (2000), Darcy-Bénard convection by Combarnous and Bories (1974) and Banu and Rees (2002) and the local thermal non-equilibrium analogue of the vertical boundary layer of Cheng and Minkowycz (1977) by Rees and Pop (2000) and Rees (2003). In all of these cited papers, local thermal non-equilibrium is modeled by two separate equations of heat transport, one for the fluid phase and one for the solid phase. The interstitial transfer

*To whom correspondence should be addressed

of heat between the phases is modeled macroscopically by a simple source/sink term which is proportional to the local temperature difference between the phases. Reviews of these matters may be found in Kuznetsov (1998) and Rees and Pop (2005). Free convection heat transfer over a vertical cylinder with variable surface temperature distributions in a porous medium was also analyzed by Shakeri *et al*. (2012). The authors assumed that the fluid and solid phases are not in local thermal equilibrium.

In the present paper we consider the combined effects of local thermal non-equilibrium (LTNE), and buoyancy due to the presence of variations of the temperature on buoyancy-induced flow from an *arbitrary* shape surface. The similarity solutions have to be solved numerically, and this forms the focus of the present paper. Our work extends the previous papers by Cheng and Minkowycz (1977) and Bagai (2003). The important novelty of this study is the similarity solution in the case of the Thermal Non-Equilibrium assumption in the porous medium, which has not been considered completely in the literature.

ANALYSIS

Consider the boundary layer flow due to free convection from an arbitrary surface embedded in a porous medium (see Figure 1). Let x, y be the Cartesian coordinates along and normal to the surface, respectively, and u, v the corresponding velocity components. Under the above assumption, the continuity equation is as follows (Bagai (2003), Nakayama and Koyama (1987)):

$$\frac{\partial(r^* u)}{\partial x} + \frac{\partial(r^* v)}{\partial y} = 0 \tag{1}$$

It is assumed that the *x*-component of velocity, i.e. *u*, is the dominant component; then by using the Boussinesq approximation and the assumptions of boundary layer, one can rewrite the equations for free convection in curvilinear system as follows (Bagai (2003), Nakayama and Koyama (1987)),

$$u = (K\beta / \nu) g_x (T_f - T_\infty) \tag{2}$$

$$\left(\rho c_p\right)_f \left(u\frac{\partial T_f}{\partial x} + v\frac{\partial T_f}{\partial y} \right) = \varepsilon k_f \frac{\partial^2 T_f}{\partial y^2} + h\left(T_s - T_f\right) \tag{3}$$

$$\left(1-\varepsilon\right) k_s \frac{\partial^2 T_s}{\partial y^2} + h\left(T_f - T_s\right) + \left(1-\varepsilon\right) q''' = 0 \tag{4}$$

where ε is the porosity, K is the permeability of the porous media, k_f and k_s are thermal conductivity of fluid and solid phases, q'' is the internal heat generation in the solid phase, β is the coefficient of thermal expansion and h is the interstitial heat transfer coefficient between the solid and fluid phases. In Eq. (1), the parameter r^* can be defined as,

$$r^* = \begin{cases} 1 & : \text{Plane Flow} \\ r(x) & : \text{Axisymmetric Flow} \end{cases}$$

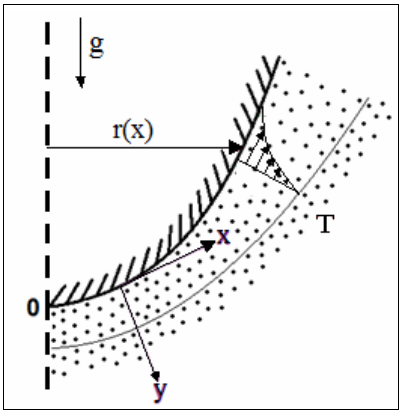

Figure 1: Shape of the surface embedded in a porous medium.

The gravity in this geometry can be defined as:

$$g_x = g\left[1 - \left(\frac{dr}{dx}\right)^2\right]^{\frac{1}{2}} \tag{5}$$

where g is total gravity and g_x is the local gravity in the boundary layer. The physical boundary conditions are also given by:

$$\begin{aligned} &At \quad y = 0 \ : \\ &v = 0 \,,\, T = T_w(x),\ T_f(x,0) = T_w(x),\ T_s(x,0) = T_w(x) \\ &As \quad y \to \infty : \\ &u(x,\infty) = 0 \,,\, T_f(x,\infty) = T_\infty \,,\, T_s(x,\infty) = T_\infty \end{aligned} \tag{6}$$

The following expressions (i.e., stream function and non-dimensional temperature) are defined to transform the governing equations:

$$\psi = \alpha r^* \left(Ra_x I\right)^{1/2} f(x,\eta) \tag{7}$$

$$T - T_\infty = \Delta T_w \theta(x,\eta) \tag{8}$$

where T is applicable for both fluid/solid phases. ΔT_w and η can be expressed as:

$$\Delta T_w = T_w(x) - T_\infty \tag{9}$$

$$\eta = \frac{y}{x}\left(\frac{Ra_x}{I}\right)^{1/2} \tag{10}$$

The new parameters are defined as:

$$I(x) = \frac{\int_0^x \Delta T_w^3 g_x r^{*2} dx}{\Delta T_w^3 g_x r^{*2} x} \tag{11}$$

$$Ra_x = \frac{K\beta g_x \Delta T_w x}{\alpha \upsilon} \tag{12}$$

$$\alpha = \frac{\varepsilon k_f}{(\rho c_p)_f} \tag{13}$$

The physical velocities can be related to the stream function as follows:

$$u = \frac{1}{r^*}\frac{\partial \psi}{\partial y} \quad , \quad v = -\frac{1}{r^*}\frac{\partial \psi}{\partial x} \tag{14}$$

The velocity components as well as temperature derivations can be obtained as follows:

$$u = \frac{\alpha f' Ra_x}{x} \tag{15}$$

$$v = -\frac{\alpha}{r^*}\left[\begin{array}{l}\left(\sqrt{Ra_x I}\right) f \dfrac{\partial r^*}{\partial x} \\ + r^*\left(\dfrac{\partial}{\partial x}\left(\sqrt{Ra_x I}\right) f + \left(\dfrac{\partial f}{\partial x}\right)\sqrt{Ra_x I}\right)\end{array}\right] \tag{16}$$

$$\frac{\partial T}{\partial x} = \frac{\partial(\Delta T_w)}{\partial x}\theta + \Delta T_w \frac{\partial \theta}{\partial x} \tag{17}$$

$$\frac{\partial T}{\partial y} = \Delta T_w \theta' \frac{1}{x}\sqrt{\frac{Ra_x}{I}} \tag{18}$$

$$\frac{\partial^2 T}{\partial y^2} = \frac{\Delta T_w}{x^2}\frac{Ra_x}{I}\theta'' \tag{19}$$

By using the above mentioned equations, the transformed governing equations are (see Appendix **A** for the detailed derivations):

$$f'' = \theta_f' \tag{20}$$

$$\begin{aligned}&\theta_f'' + \left(\frac{1}{2} - nI\right) f\theta_f' - nIf'\theta_f + \frac{x^2 I}{k_f Ra_x} h\left(\theta_s - \theta_f\right) \\ &= Ix\left(f'\frac{\partial \theta}{\partial x} - \theta'\frac{\partial f}{\partial x}\right)\end{aligned} \tag{21}$$

$$\begin{aligned}&\theta_s'' + \frac{1}{(1-\varepsilon)k_s}\frac{x^2 I}{\Delta T_w Ra_x} h\left(\theta_f - \theta_s\right) \\ &+ \frac{1}{k_s}\frac{x^2 I}{\Delta T_w Ra_x} q''' = 0\end{aligned} \tag{22}$$

where n is defined as:

$$n(x) = \frac{x}{\Delta T_w}\frac{\partial(\Delta T_w)}{\partial x} = \frac{d\,[\ln \Delta T_w]}{d\,[\ln x]} \tag{23}$$

To obtain the similarity solution, the convective heat transfer coefficient (h) and heat source in the solid phase (q''') are now defined as:

$$h = \frac{\varepsilon k_f}{(1+3\lambda)}\frac{Ra_x}{x^2 I} e^{\left(\frac{\eta}{\sqrt{1+3\lambda}}\right)} \tag{24}$$

$$q''' = \frac{k_s \Delta T_w}{(1+3\lambda)}\frac{Ra_x}{x^2 I} e^{\left(-\frac{\eta}{\sqrt{1+3\lambda}}\right)} \tag{25}$$

The transformed boundary conditions are:

$$\begin{aligned}&At\ \eta = 0: \quad f(0) = 0,\ f'(0) = 0, \\ &As\ \eta \to \infty: \ f'(\infty) = 0,\ f''(\infty) = 0,\ f'''(0) = 0.\end{aligned} \tag{26}$$

When the values of $\frac{\partial f}{\partial x}$ and $\frac{\partial f'}{\partial x}$ are small, the right hand side of equation (21) may be neglected and the governing equations can be obtained as:

$$f' = \theta_f \tag{27}$$

$$\begin{aligned}&\theta_f'' + \left(\frac{1}{2} - nI\right) f\theta_f' - nIf'\theta_f \\ &+ \frac{1}{(1+3\lambda)} e^{\left(\frac{\eta}{\sqrt{1+3\lambda}}\right)}\left(\theta_s - \theta_f\right) = 0\end{aligned} \tag{28}$$

$$\theta_s'' + \frac{k_{eff}}{(1+3\lambda)} e^{\left(\frac{\eta}{\sqrt{1+3\lambda}}\right)} \left(\theta_f - \theta_s\right) + \frac{1}{(1+3\lambda)} e^{\left(-\frac{\eta}{\sqrt{1+3\lambda}}\right)} = 0 \tag{29}$$

Equation (27) is obtained by integration of equation (20) under the boundary conditions specified by Eq. (26). k_{eff} is also the fluid-to-solid conductivity ratio as:

$$k_{eff} = \frac{\varepsilon k_f}{(1-\varepsilon)k_s} \tag{30}$$

Now, we can define the new parameter ξ as:

$$\xi = \int_0^x g_x r^{*2} dx, \tag{31}$$

By considering Equations (11), (23) and (31), and assuming $\Delta T_w \propto \xi^{\lambda}$, one would have (see Appendix B for the detailed derivations):

$$n\,I = \frac{d\ln(\Delta T_w)}{d\ln(x)} \times \frac{\int_0^{\xi} \Delta T_w{}^3 d\xi}{\Delta T_w{}^3 \xi} = \frac{\lambda}{(1+3\lambda)}. \tag{32}$$

In the above equation, $d\xi = g_x r^{*2} dx$. In other words, to have a similarity solution, the temperature changes around the surface should be defined as an expansion function:

$$\Delta T_w \propto \xi^{\lambda} \tag{33}$$

The coupled equations can be solved numerically. Thus, the transformed governing equations and the associated boundary conditions are solved by means of the 4th order Runge-Kutta method along with the Shooting Method technique (see: Burden and Faires (2010), Chapter 11). 100 Uniform grid-points are used in the η direction. The iteration process continues until the convergence criterion for all the variables, 10^{-5}, is achieved. The correct selection of η_{max} is important to ensure that: i) the boundary layer remains within the computational domain; ii) the selection of the distance from the surface for applying the infinity boundary does not affect the calculated results such as wall shear stress and the Nusselt number. Thus, the solution (such as the boundary layer) should asymptotically tend to zero at large values of η.

GEOMETRICAL STATEMENT: SPECIAL CASES

Various surface geometries with different thermal boundary conditions are considered as follows, considering Eq. (31):

$$\xi = gx, \quad \text{Vertical Plate} \tag{34}$$

$$\xi = gr(1-\cos\Phi), \quad \text{Horizontal Cylinder} \tag{35}$$

$$\xi = gr^3\left(\frac{1}{3}\cos^3\Phi - \cos\Phi + \frac{2}{3}\right), \quad \text{Sphere} \tag{36}$$

where $\Phi = \sin^{-1}\left(\frac{x}{r}\right)$, r is the radius of the cylinder or sphere, and x is the distance from the stagnation point. The local surface heat flux is calculated as:

$$q_w = -\varepsilon k_f \left.\frac{\partial T_f}{\partial y}\right|_{y=0} - (1-\varepsilon)k_s \left.\frac{\partial T_s}{\partial y}\right|_{y=0} \tag{37}$$

and the dimensionless local heat flux is defined as:

$$q^* = \left(\frac{q_w L_r}{\Delta T_{wr} \varepsilon k_f}\right)\left(\frac{K\beta \Delta T_{wr} g L_r}{\alpha \upsilon}\right)^{-\frac{1}{2}} \tag{38}$$

where T_{wr} is the wall ambient temperature difference at the trailing edge or the rear stagnation point and L_r is the reference length. Equation (38) for the aforementioned geometries, described by Eqs. (34)-(36), can be written as follows:

$$q^* = \left[-\theta_f' - \frac{\theta_s'}{k_{eff}}\right](1+3\lambda)^{\frac{1}{2}}\left(\frac{x}{L_r}\right)^{\frac{3\lambda-1}{2}}, \tag{39}$$

Vertical Plate

$$q^* = \left[-\theta_f' - \frac{\theta_s'}{k_{eff}}\right](1+\cos\Phi)^{\frac{1}{2}}\left(\frac{1-\cos\Phi}{2}\right)^{\frac{3\lambda}{2}}, \tag{40}$$

Horizontal Cylinder

$$q^* = \left[-\theta_f' - \frac{\theta_s'}{k_{eff}} \right] \left(\frac{3}{2+\cos\Phi} \right)^{\frac{1}{2}} \left(1+\cos\Phi\right) \left(\frac{\cos^3\Phi - 3\cos\Phi + 2}{4} \right)^{\frac{3\lambda}{2}}, \text{ Sphere} \quad (41)$$

VALIDATION

When k_{eff} is infinite, it means that the porous medium is in the equilibrium condition. In this condition, the value of $\varepsilon k_f >> (1-\varepsilon)k_s$ and therefore the fluid and solid phases are in the thermal equilibrium condition. A validation study was done by comparing the numerical results with those presented by Cheng and Minkowycz (1977). In this reference, the authors investigated a vertical plate in a porous medium in the case of the thermal equilibrium condition. By choosing a large value for k_{eff}, the thermal equilibrium condition is clearly satisfied. The related calculations are presented in Table 1. According to the results, which are shown in the table; our solution methods as well as the numerical assumptions are accurate.

Table 1: Comparing the values of q^* in a vertical plate for $k_{eff} = 1000$ with the numerical results of Cheng and Minkowycz (1977).

λ	Cheng and Minkowycz (1977)	Present Results
0	0.4440	0.44397
1/5	0.5943	0.59429
1/4	0.6303	0.62687
1/3	0.6788	0.67799
1/2	0.7615	0.77075
3/4	0.8926	0.892795
1	1.001	1.00051

The results were also checked with those presented by Bagai (2003), who considered a porous medium in the thermal equilibrium condition including heat generation in both the fluid/solid phases. In addition, the author presented the values of heat flux when there was no heat generation inside the phases. In order to have thermal equilibrium, we omitted the heat generation in the solid phase and assumed that k_{eff} had a large value. Then, the results obtained can be compared with Bagai (2003) for two different geometries, namely the ''horizontal cylinder'' and ''sphere'' shapes. The results are shown in Figure (2). According to the results, our method as well as the numerical assumptions are accurate.

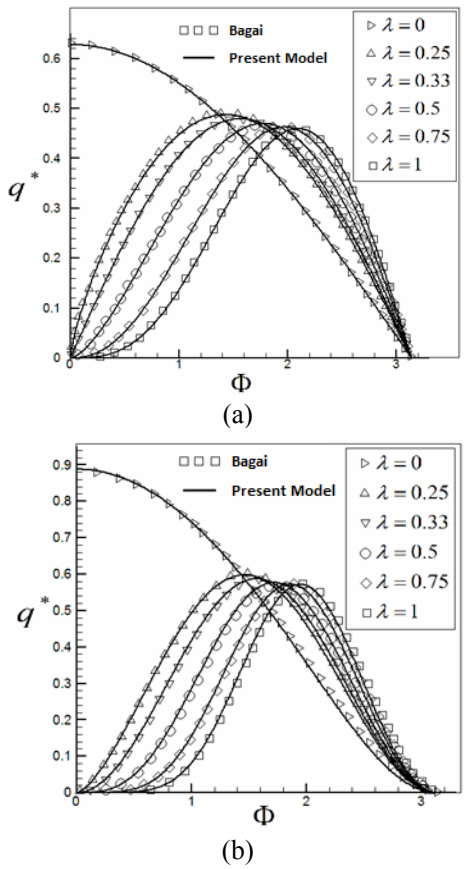

Figure 2: Comparison with Bagai (2003) in the case of the thermal equilibrium condition, for k_{eff}=1000, without internal heat generation for (a) cylinder, (b) sphere.

RESULTS AND DISCUSSION

The present model can be employed for various values of λ for a vertical heated plate in a porous medium. As presented in Table 2, different values of k_{eff} are considered and the related heat flux, i.e., q^*, is reported. The results obtained showed that, upon increasing the fluid-to-solid conductivity ratio, i.e., k_{eff}, the surface heat flux is decreased.

As presented in the similarity equations, the value of λ=0 is related to a constant temperature of the surface. As the value of λ increases, the heat transfer rate, denominated by q^*, is also increased. This is obviously related to the definition of the temperature difference, ΔT_w, present in Eq. (33). As indicated in

this equation, increasing the value of λ leads to an increase in the value of the surface temperature and therefore clearly affected the heat transfer to the working fluid.

Table 2: q^* for Vertical Plate for different values of λ and (a) $k_{eff}=0.1$ (b) $k_{eff}=1$ (c) $k_{eff}=10$.

λ	q^*
0	1.4718
1/5	1.9339
1/4	2.0303
1/3	2.179
1/2	2.4404
3/4	2.7686
1	3.0442

(a)

λ	q^*
0	0.6232
1/5	0.8272
1/4	0.8709
1/3	0.9391
1/2	1.0616
3/4	1.2204
1	1.3586

(b)

λ	q^*
0	0.4652
1/5	0.6224
1/4	0.6565
1/3	0.7099
1/2	0.8067
3/4	0.934
1	1.0462

(c)

The definition of k_{eff} in the governing equations clearly reflects the effects of the two phase approach in our simulation, which was not introduced in the work of Cheng and Minkowycz (1977).

The values of heat flux, q^*, as a function of k_{eff} are shown in Figure (3) for different values of λ. The results are related to three geometries, i.e., vertical plate, horizontal cylinder and sphere.

According to the results obtained, it is found that, in all geometries, the dimensionless local heat flux increases with k_{eff} for various values of λ. As shown in Figure (3), the value of $\Phi=\sin^{-1}(x/r)=\pi/2$, which is related to a fixed point on the body. The values of the dimensionless local heat flux for a horizontal cylinder are also shown in Figure 4. The figures are presented for three different values of k_{eff}=0.1, 1 and 10. The value of λ=0 is related to a constant temperature of the cylinder surface. The horizontal axis is selected as $\phi=\sin^{-1}(x/r)$, where r is the radius of the cylinder, and x is distance from the stagnation point. As shown in this figure, there is a maximum (or minimum) value for the surface heat flux (q^*) when the temperature of the body is not constant ($\lambda\neq 0.$). This extremum location is strongly related to the values of the fluid-to-solid conductivity ratio. Similarly, the results obtained for a hot sphere in a porous medium are shown in Figure (5).

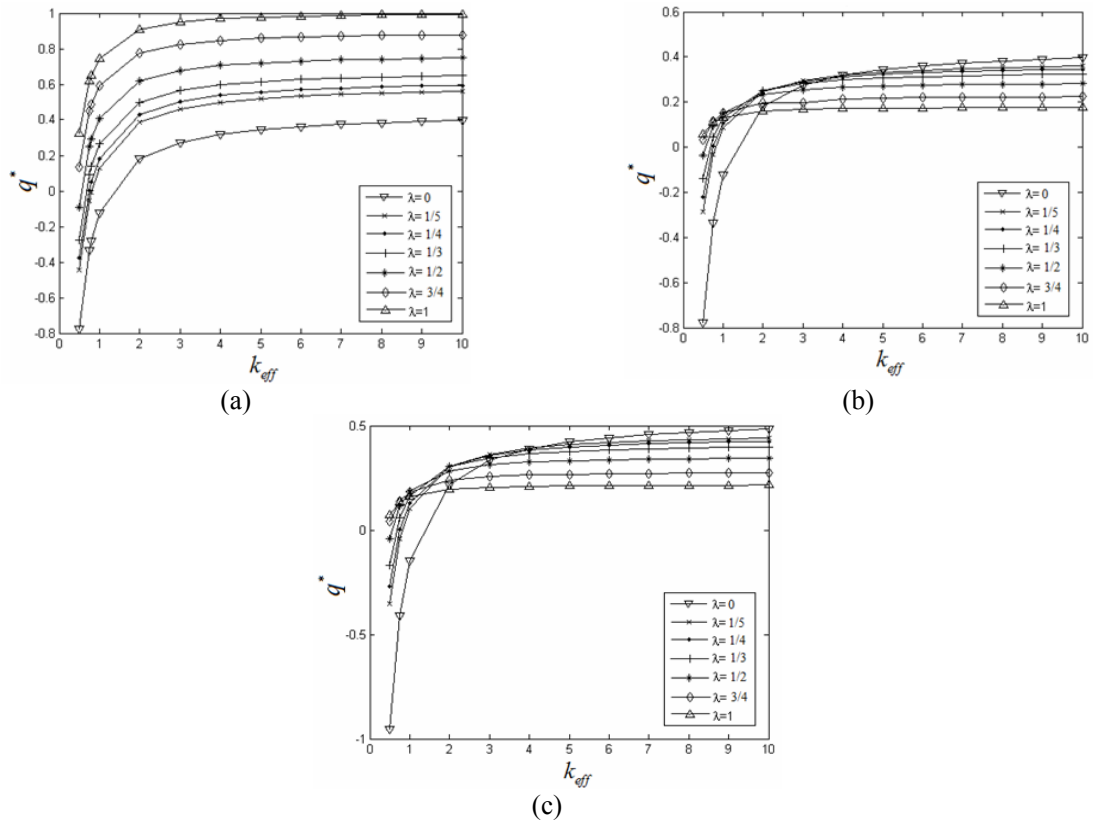

(a) (b)

(c)

Figure 3: Local heat flux for different values of λ. (a) Vertical Plate, (b) Horizontal Cylinder with internal heat generation and $\phi=\pi/2$, (c) Sphere with internal heat generation and $\phi=\pi/2$.

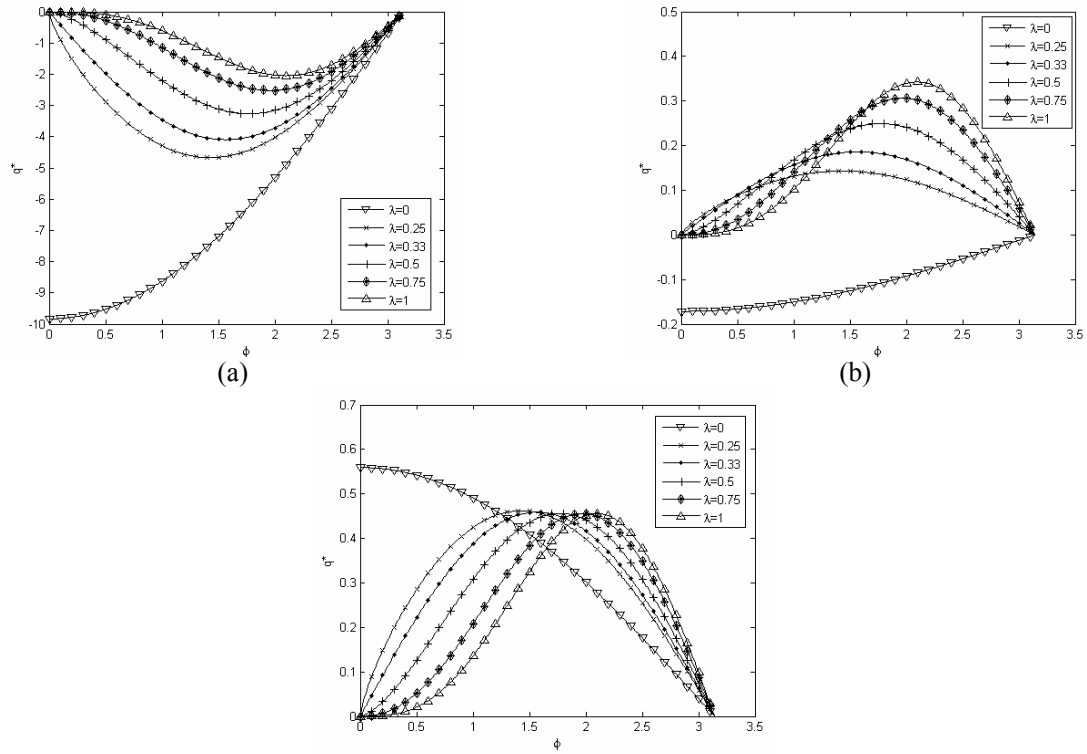

Figure 4: Local heat flux for a horizontal cylinder with internal heat generation in the solid phase (a) $k_{eff} = 0.1$, (b) $k_{eff} = 1$, (c) $k_{eff} = 10$.

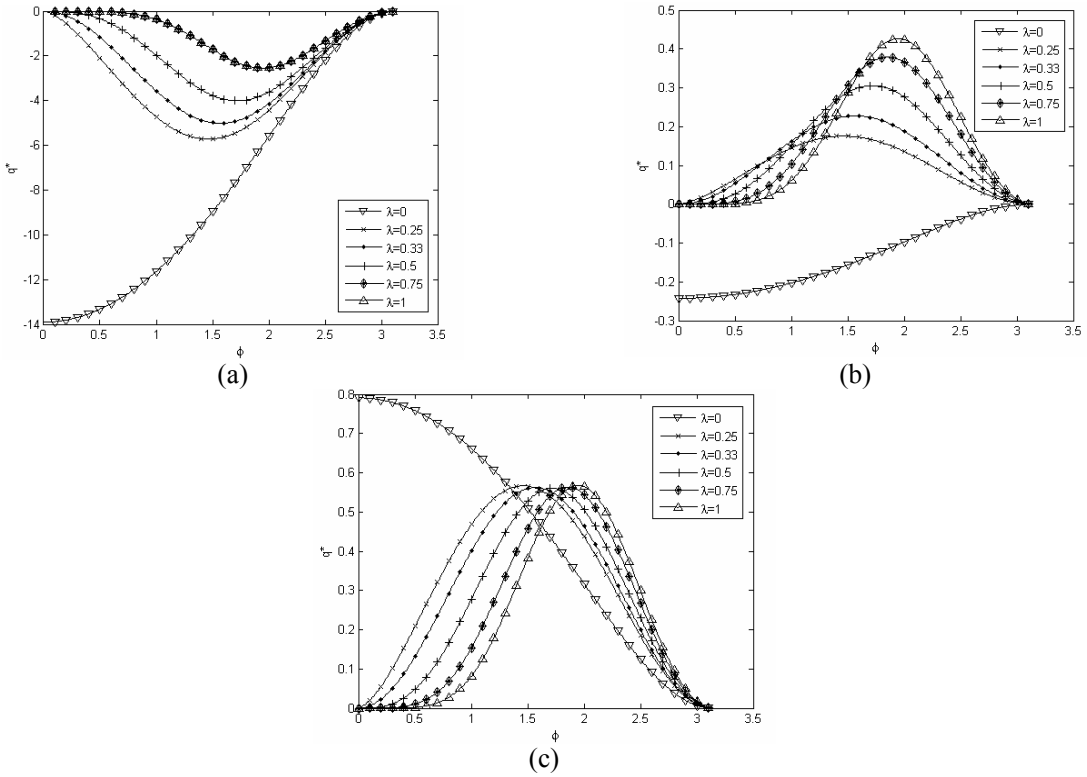

Figure 5: Local heat flux for a sphere with internal heat generation in the solid phase (a) $k_{eff} = 0.1$, (b) $k_{eff} = 1$, (c) $k_{eff} = 10$.

CONCLUSION AND HIGHLIGHTS

The study of the natural convection flow and heat transfer from hot surfaces in a porous medium has been of considerable interest in energy-related engineering problems. This paper is concerned with the free convection heat transfer over an *arbitrary* hot surface in a porous medium. Mathematical derivation of a similarity solution for an *arbitrary* geometry in the heat transfer analysis is the main novelty of the present study. The equations obtained are solved and the local heat flux is presented for three types of shapes, i.e., vertical plate, horizontal cylinder and sphere. The present model can be employed for analysis of heat transfer induced by *arbitrary-shape* surfaces.

NOMENCLATURE

List of Symbols

c_p	specific heat at constant pressure of the fluid
f	dimensionless stream function
g	acceleration due to gravity
k	thermal conductivity
K	permeability
h	coefficient of convection heat transfer
q'''	internal heat generation per unit volume
q_w	local surface heat flux
q^*	local heat flux
r	function representing wall geometry
Ra_x	local Rayleigh number
T	temperature
u,v	velocity components in the x and y directions
x,y	boundary layer coordinates

Greek Symbols

α	thermal diffusivity
β	coefficient of thermal expansion
η	similarity variable
θ	dimensionless temperature
λ	exponent associated with the wall temperature increase
ε	porosity
ρ	density of fluid phase
υ	kinematic viscosity
ψ	stream function

Subscripts

eff	Effective
f	fluid
s	solid
w	wall condition
∞	ambient condition

Superscript

'	denotes derivative with respect to η

REFERENCES

Bagai, S., Similarity solutions of free convection boundary layers over a body of arbitrary shape in a porous medium with internal heat generation. Int. Comm. Heat Mass Transfer, 30, 997 (2003).

Banu, N., Rees, D. A. S., The onset of Darcy-Bénard convection using a thermal nonequilibrium model. Int. J. Heat Mass Transfer, 45, 2221 (2002).

Baytaş, A. C. and Pop, I., Free convection in a square porous cavity using a thermal nonequilibrium model. International Journal of Thermal Sciences, 41, 861 (2002).

Burden, R. L., Faires, J. D., Numerical Analysis. 9th Edition, Brooks/Cole, Cengage Learning, Chapter 11 (2010).

Cheng, P., Minkowycz, W. J., Free convection about a vertical flat plate embedded in a porous medium with application to heat transfer from a dike. J. Geophys. Res., 82, 2040 (1977).

Combarnous, M., Bories, S., A modelization of natural convection inside a horizontal porous layer using a solid-fluid transfer coefficient. Int. J. Heat Mass Transfer, 17, 505 (1974).

Kuznetsov, A. V., Thermal Nonequilibrium Forced Convection in Porous Media. In: Transport Phenomena in Porous Media, (D. B. Ingham and I. Pop, Eds.), Pergamon, Oxford, UK (1998).

Mohamad, A. A., Nonequilibrium natural convection in a differentially heated cavity filled with a porous matrix. Trans. ASME J. Heat Transfer, 122, 380 (2000).

Nakayama, A., Koyama, H., Free convective heat transfer over a nonisothermal body of arbitrary shape embedded in a fluid-saturated porous medium. Journal of Heat Transfer (Trans. of the ASME), 109, 125 (1987).

Rees, D. A. S., Vertical free convective boundary-layer flow in a porous medium using a thermal

nonequilibrium model: Elliptical effects. Journal of Applied Mathematics and Physics (JAMP), 54, 437 (2003).

Rees, D. A. S., Bassom, A. P., The radial injection of a hot fluid into a cold porous medium: The effects of local thermal non-equilibrium. Computational Thermal Sciences, 2(3), 221 (2010).

Rees, D. A. S., Bassom, A. P., Siddheshwar, P. G., Local thermal non-equilibrium effects arising from the injection of a hot fluid into a porous medium. Journal of Fluid Mechanics, 594, 379 (2008).

Rees, D. A. S., Pop, I., Vertical free convective boundary-layer flow in a porous medium using a thermal nonequilibrium model. Journal of Porous Media, 3, 31 (2000).

Rees, D. A. S., Pop, I., Local Thermal Nonequilibrium in Porous Medium Convection. In: Transport Phenomena in Porous Media III, (D. B. Ingham and I. Pop, Eds.), Pergamon, Oxford, UK, 147 (2005).

Shakeri, E., Nazari, M., Kayhani, M. H., Free convection heat transfer over a vertical cylinder in a saturated porous medium using a local thermal non-equilibrium model. Transport in Porous Media, 93, 453 (2012).

APPENDIX A

Governing equations:

$$\frac{\partial(r^* u)}{\partial x}+\frac{\partial(r^* v)}{\partial y}=0$$

$$u=\left(\frac{K\beta}{\vartheta}\right)g_x(T_f-T_\infty)$$

$$\left(\rho c_p\right)_f\left(u\frac{\partial T_f}{\partial x}+v\frac{\partial T_f}{\partial y}=\varepsilon K_f\frac{\partial^2 T_f}{\partial y^2}+h(T_s-T_f\right)$$

$$(1-\varepsilon)K_s\frac{\partial^2 T_s}{\partial y^2}+h\left(T_f-T_s\right)+(1-\varepsilon)q'''=0$$

The following equations are defined:

$$\Psi=\propto r^*\left(Ra_x I\right)^{1/2} f(x,\eta)$$

$$T-T_\infty=\Delta T_w\theta(x,\eta)$$

$$\eta=\frac{y}{x}\left(\frac{Ra_x}{I}\right)^{1/2}$$

$$\propto=\frac{\varepsilon K_f}{(\rho c_p)_f}$$

and;

$$u=\frac{1}{r^*}\frac{\partial\Psi}{\partial y}$$

$$v=-\frac{1}{r^*}\frac{\partial\Psi}{\partial x}$$

Therefore, the following equations are derived based on the definition of f, θ and Ra_x:

$$u=\frac{\propto f' Ra_x}{x}$$

$$v=-\frac{\propto}{r^*}\left[\sqrt{Ra_x I}f\frac{\partial r^*}{\partial x}+r^*(\frac{\partial}{\partial x}\left(\sqrt{Ra_x I}\right)f+\left(\frac{\partial f}{\partial x}\right)\sqrt{Ra_x I}\right]$$

$$\frac{\partial T}{\partial x}=\frac{\partial(\Delta T_w)}{\partial x}\theta+\Delta T_w\frac{\partial\theta}{\partial x}$$

$$\frac{\partial T}{\partial y}=\Delta T_w\theta'\frac{1}{x}\sqrt{\frac{Ra_x}{I}}$$

$$\frac{\partial^2 T}{\partial y^2}=\frac{\Delta T_w}{x^2}\frac{Ra_x}{I}\theta''$$

The energy equation for the fluid phase is as follows:

$$\left(\rho c_p\right)_f\left(u\frac{\partial T_f}{\partial x}+v\frac{\partial T_f}{\partial y}\right)=\varepsilon K_f\frac{\partial^2 T_f}{\partial y^2}+h(T_s-T_f)$$

By substituting the required parameters (such as *u*, *v* and gradients of *T*) into the energy equation, one would have:

$$\frac{\varepsilon K_f Ra_x}{x}\frac{\partial(\Delta T_w)}{\partial x}f'\theta_f+\frac{\varepsilon K_f Ra_x}{x}\Delta T_w f'\frac{\partial\theta_f}{\partial x}-\frac{\varepsilon K_f Ra_x}{x}\Delta T_w\frac{1}{r^*}\frac{\partial r^*}{\partial x}f\theta_f{}'-\frac{\varepsilon K_f\Delta T_w}{x}\left(\frac{Ra_x}{I}\right)^{1/2}\frac{\partial\left(Ra_xI\right)^{1/2}}{\partial x}f\theta_f{}'$$

$$-\frac{\varepsilon K_f Ra_x}{x}\Delta T_w\theta_f{}'\frac{\partial f}{\partial x}=\frac{\varepsilon K_f Ra_x\Delta T_w}{x^2I}\theta_f{}''+\Delta T_w h(\theta_s-\theta_f)$$

$$\left(\frac{x^2I}{K_f\Delta T_w Ra_x}\right)\left(\frac{K_f Ra_x}{x}\frac{\partial(\Delta T_w)}{\partial x}\right)f'\theta_f+\left(\frac{x^2I}{K_f\Delta T_w Ra_x}\right)\left(\frac{K_f Ra_x\Delta T_w}{x}\right)f'\frac{\partial\theta_f}{\partial x}$$

$$-\left(\frac{x^2I}{K_f\Delta T_w Ra_x}\right)\left(\frac{K_f Ra_x\Delta T_w}{xr^*}\frac{\partial r^*}{\partial x}\right)f\theta_f{}'-\left(\frac{x^2I}{K_f\Delta T_w Ra_x}\right)\left(\frac{K_f\Delta T_w}{x}\left(\frac{Ra_x}{I}\right)^{1/2}\frac{\partial\left(Ra_xI\right)^{1/2}}{\partial x}\right)f\theta_f{}'$$

$$-\left(\frac{x^2I}{K_f\Delta T_w Ra_x}\right)\left(\frac{K_f Ra_x\Delta T_w}{x}\right)\theta_f{}'\frac{\partial f}{\partial x}=\theta_f{}''+\left(\frac{x^2I}{K_f\Delta T_w Ra_x}\right)\left(\frac{\Delta T_w h}{\varepsilon}\right)(\theta_s-\theta_f)$$

and, after some mathematical manipulation:

$$\theta_f{}''+\left(\frac{x^2I}{K_f Ra_x}\right)\left(\frac{h}{\varepsilon}\right)(\theta_s-\theta_f)-I\frac{\left(\frac{\partial(\Delta T_w)}{\Delta T_w}\right)}{\left(\frac{\partial x}{x}\right)}f'\theta_f+\left(\frac{xI}{r^*}\frac{\partial r^*}{\partial x}+\frac{xI}{Ra_x}\frac{\partial\left(Ra_xI\right)^{1/2}}{\partial x}\right)f\theta_f{}'=Ix\left(f'\frac{\partial\theta_f}{\partial x}-\theta_f{}'\frac{\partial f}{\partial x}\right)$$

Also, on the right hand side of the above equation, we can derive $\frac{\partial\left(Ra_xI\right)^{0.5}}{\partial x}$ as follows:

$$\frac{\partial\left(Ra_xI\right)}{\partial x}=\frac{K\beta}{\alpha\vartheta}\left[\frac{\Delta T_w{}^3gr^{*2}\left(\Delta T_w{}^2r^{*2}\right)-\left(\Delta T_w{}^2r^{*2}\right)'\int\Delta T_w{}^3gr^{*2}dx}{\left(\Delta T_w{}^2r^{*2}\right)^2}\right]=\frac{K\beta\Delta T_w g}{\alpha\vartheta}-\frac{K\beta}{\alpha\vartheta}\frac{I\left(\Delta T_w{}^2r^{*2}\right)'g}{\left(\Delta T_w r^{*2}\right)}$$

$$=\frac{Ra_x}{x}-Ra_xI\left(\frac{2\Delta T_w\frac{\partial(\Delta T_w)}{\partial x}r^{*2}+2r^*\frac{\partial r^*}{\partial x}\Delta T_w{}^2}{\left(\Delta T_w{}^2r^{*2}\right)}\right)=\frac{Ra_x}{x}-Ra_xI\left(\frac{2}{\Delta T_w}\frac{\partial(\Delta T_w)}{\partial x}+\frac{2}{r^*}\frac{\partial r^*}{\partial x}\right)$$

$$\frac{\partial\left(Ra_xI\right)^{1/2}}{\partial x}=\frac{1}{2\left(Ra_xI\right)^{1/2}}\left[\frac{Ra_x}{x}-Ra_xI\left(\frac{2}{\Delta T_w}\frac{\partial(\Delta T_w)}{\partial x}+\frac{2}{r^*}\frac{\partial r^*}{\partial x}\right)\right]$$

Therefore, after some manipulations, one would have:

$$\theta_f{}''+\left(\frac{x^2I}{K_f Ra_x}\right)\left(\frac{h}{\varepsilon}\right)(\theta_s-\theta_f)-nIf'\theta_f+\frac{xI}{r^*}\frac{\partial r^*}{\partial x}+\frac{1}{2}-\frac{xI}{\Delta T_w}\frac{\partial(\Delta T_w)}{\partial x}-\frac{xI}{r^*}\frac{\partial r^*}{\partial x})f\theta_f{}'=Ix\left(f'\frac{\partial\theta_f}{\partial x}-\theta_f{}'\frac{\partial f}{\partial x}\right)$$

$$\theta_f{}''+\left(\frac{x^2I}{K_f Ra_x}\right)\left(\frac{h}{\varepsilon}\right)(\theta_s-\theta_f)-nIf'\theta_f+\left(\frac{1}{2}-nI\right)f\theta_f{}'=Ix\left(f'\frac{\partial\theta_f}{\partial x}-\theta_f{}'\frac{\partial f}{\partial x}\right)$$

When the RHS is small, the right hand side of the above equation may be neglected and the governing equations can be obtained as,

$$\theta_f'' - nIf'\theta_f + \left(\frac{1}{2} - nI\right) f\theta_f' \left[\frac{1}{(1+3\lambda)} e^{\left(\frac{\eta}{\sqrt{1+3\lambda}}\right)}\right]\left(\theta_s - \theta_f\right) = 0$$

where,

$$h = \frac{\varepsilon K_f}{(1+3\lambda)} \frac{Ra_x}{x^2 I} e^{\left(\frac{\eta}{\sqrt{1+3\lambda}}\right)}$$

Similarly, for the solid phase energy equation:

$$(1-\varepsilon) K_s \frac{\partial^2 T_s}{\partial y^2} + h\left(T_f - T_s\right) + (1-\varepsilon) q''' = 0$$

$$(1-\varepsilon) K_s \frac{\Delta T_w}{x^2} \frac{Ra_x}{I} \theta_s'' + \frac{\varepsilon K_f}{(1+3\lambda)} \frac{Ra_x}{x^2 I} e^{\left(\frac{\eta}{\sqrt{1+3\lambda}}\right)} + (1-\varepsilon) q''' = 0$$

The heat generation is defined as:

$$q''' = \frac{K_s \Delta T_w}{(1+3\lambda)} \frac{Ra_x}{x^2 I} e^{\left(\frac{-\eta}{\sqrt{1+3\lambda}}\right)}$$

Therefore,

$$\theta_s'' + \left(\frac{\varepsilon K_f}{(1-\varepsilon) K_s}\right) \frac{1}{(1+3\lambda)} e^{\left(\frac{\eta}{\sqrt{1+3\lambda}}\right)} \left(\theta_f - \theta_s\right) + \frac{1}{(1+3\lambda)} e^{\left(\frac{-\eta}{\sqrt{1+3\lambda}}\right)} = 0$$

$$K_0 = \frac{\varepsilon K_f}{(1-\varepsilon) K_s}$$

$$\theta_s'' + K_0 \frac{1}{(1+3\lambda)} e^{\left(\frac{\eta}{\sqrt{1+3\lambda}}\right)} \left(\theta_f - \theta_s\right) + \frac{1}{(1+3\lambda)} e^{\left(\frac{-\eta}{\sqrt{1+3\lambda}}\right)} = 0$$

APPENDIX B

$$n\,I = \frac{d\ln\left(\Delta T_w\right)}{d\ln(x)} \times \frac{\int_0^{\xi} \Delta T_w{}^3 d\xi}{\Delta T_w{}^3 \xi} = \frac{d\ln\left(\Delta T_w\right)}{d\ln(x)} \times \frac{\int_0^{x} \Delta T_w{}^3 g_x r^{*2} dx}{\Delta T_w{}^3 g_x r^{*2} x},$$

We set $\left(\Delta T_w\right) = C\xi^{\lambda}$

$$n\,I = \frac{d\ln\left(C\xi^{\lambda}\right)}{\frac{dx}{x}} \times \frac{\int_0^{\xi} (C\xi^{\lambda})^3 d\xi}{(C\xi^{\lambda})^3 g_x r^{*2} x} = \frac{\lambda\, d(\ln\xi)}{d\xi} \frac{\int_0^{\xi} \xi^{3\lambda} d\xi}{\xi^{3\lambda}} = \frac{\lambda\, d(\ln\xi)}{d\xi} \frac{\xi^{3\lambda+1}}{\xi^{3\lambda}(1+3\lambda)}$$

It is obvious that: $d\xi = \xi\, d(\ln\xi)$

Therefore,

$$n\,I = \frac{\lambda\, d(\ln\xi)}{d\xi} \frac{\xi^{3\lambda+1}}{\xi^{3\lambda}(1+3\lambda)} = \frac{\lambda}{1+3\lambda}$$